Cancer Cell Radiobiological Studies Using In-House-Developed α-Particle Irradiator.

Nilsson, Jenny; Bauden, Monika; Nilsson, Jonas; Strand, Sven-Erik; Elgqvist, Jörgen

Published in:
Cancer Biotherapy & Radiopharmaceuticals

DOI:
10.1089/cbr.2015.1895

2015

Cancer Cell Radiobiological Studies Using In-House Developed Alpha-Particle Irradiator

Jenny Nilsson[1]; Monika P. Bauden[2]; Jonas M. Nilsson[3]; Sven-Erik Strand[4]; Jörgen Elgqvist[4]*

[1]Department of Radiation Physics, Gothenburg University, Gothenburg, Sweden
[2]Department of Surgery, Institution of Clinical Sciences, Lund University, Lund, Sweden
[3]Department of Medical Radiation Physics, Lund University, Malmö, Sweden
[4]Department of Medical Radiation Physics, Institution of Clinical Sciences, Lund University, Lund, Sweden

Word count: 6200 (excluding references)

Running title: Alpha-Particle Irradiation of Cancer Cells.

***Correspondence to**: Jörgen Elgqvist, PhD, Associate Professor, Department of Medical Radiation Physics, Institution of Clinical Sciences, Lund University, Barngatan2B, 221 85 Lund, Sweden. E-mail: jorgen.elgqvist@med.lu.se; jorgen.elgqvist@gmail.com

ABSTRACT

An alpha-particle irradiator, enabling high-precision irradiation of cells for *in-vitro* studies, has been constructed. The irradiation source was a ^{241}Am source, on which well inserts containing cancer cells growing in monolayer were placed. The total radioactivity, uniformity, and alpha-particle spectrum were determined by use of HPGe-detector, Gafchromic™-dosimetry film, and PIPS®-detector measurements, respectively. Monte Carlo simulations were used for dosimetry. Three prostate cancer (LNCaP, DU145, PC3) and three pancreatic cancer (Capan-1, Panc-1, BxPC-3) cell lines were irradiated by alpha particles to the absorbed doses 0, 0.5, 1, and 2 Gy. For reference, cells were irradiated using ^{137}Cs to the absorbed doses 0, 1, 2, 4, 6, 8, and 10 Gy. Radiation sensitivity was estimated using a tetrazolium salt-based colorimetric assay with absorbance measurements at 450 nm. The relative biological effectiveness for alpha particles relative to gamma irradiation at 37% cell survival for the LNCaP, DU145, PC3, Capan-1, Panc-1, and BxPC-3 cells were 7.9 ± 1.7, 8.0 ± 0.8, 7.0 ± 1.1, 12.5 ± 1.6, 9.4 ± 0.9, and 6.2 ± 0.7, respectively. The results show the feasibility of constructing a desk-top alpha-particle irradiator, as well as indicate that both prostate and pancreatic cancers are good candidates for further studies of alpha-particle radioimmunotherapy.

Key words: Pancreatic cancer; Prostate cancer; High-LET radiation; Dosimetry; Radioimmunotherapy

INTRODUCTION

Based on the legendary work on radioactivity by Antoine Henri Becquerel published in Comptes Rendus in 1896, Ernest Rutherford discovered the alpha particle in 1899 during his famous study of the radiation emitted from uranium, and the electrical conduction produced by it (1) (2). This type of radiation has ever since been under investigation regarding its various characteristics and possible applications. Especially during the last two decades, focused attention in the field of therapeutic nuclear medicine has been directed towards alpha-particle emitters intended for targeted alpha therapy (TAT) against disseminated microscopic cancer. In such studies, alpha-particle emitters such as ^{225}Ac, ^{223}Ra, ^{211}At, ^{213}Bi, and ^{212}Bi have been used (3) (4) (5) (6) (7) (8). The distinctive feature of alpha particles, compared to for example gamma radiation or beta particles, are their ability to create densely ionizing tracks when passing through tissue (9). This is often expressed as the linear energy transfer (LET) and is a measure of the radiation's ability to transfer energy to the surrounding media per unit length travelled by the particle (10). Alpha particles have a mean LET in the range of 100 keV/µm. The LET vary along the Bragg curve, depending on the initial energy of the alpha particle, from initially ~50 to ~250 keV/µm at the Bragg peak. By comparison, gamma rays from ^{137}Cs or beta particles from ^{177}Lu, ^{131}I, or ^{90}Y, have a LET in the range of 0.3 keV/µm. Auger electrons, emitted from for example ^{111}In or ^{125}I, have a LET range in the order of 10−25 keV/µm during their cascade decay (11). Another feature that differs between alpha particles, beta particles and Auger electrons is the range. In tissue, alpha particles have a range in the order of 50−100 µm, while beta particles and Auger electrons have an average range at the millimeter and nanometer scale, respectively. Hence, alpha particles have certain special features and are therefore a useful alternative when evaluating new radioimmunotherapeutic treatment strategies against cancer *in vivo* or in the clinic, or when investigating the inherent radiation sensitivity of different cells *in vitro*.

Radioimmunotherapy (RIT) has developed during the past decades resulting in two FDA-approved drugs using beta-particle emitters; Zevalin® and Bexxar® (*i.e*. ^{90}Y Ibritumomab and ^{131}I Tositumomab, respectively), both used to treat refractory low-grade B-cell non-Hodgkin lymphomas (12) (13) (14) (15). Another newly FDA-approved drug is Xofigo®, which is based on an alpha-particle emitter (16). Although strictly speaking not a RIT approach, it is a targeted treatment against metastatic bone-localized prostate cancer. This drug consists of ^{223}Ra-dichlorid that is used to treat symptomatic bone metastases of castration resistant prostate cancer. The targeting is achieved because the substance is mimicking calcium, and therefore selectively targets high metabolic bone structures with involved bone metastases by complex formation with bone minerals.

In this study we have developed a bench-top easy to use external alpha-particle irradiator and thereby enabling the inclusion of alpha particles during studies of inherent radiation sensitivity of cancer cells. The design of the irradiator is relatively low cost and could be implemented in almost any laboratory. Another advantage of this irradiator is the detailed description of the Monte Carlo (MC) modeling for the dosimetry and the usage of the open source MC code GATE, using the well validated and documented GEANT4 physics. In order to construct such an irradiator, that once calibrated can be used over a long time period, we have chosen the alpha-particle emitter ^{241}Am. This radionuclide has a half-life of 432.6 y and emits alpha particles of energies 5.48 MeV (84.5%), 5.44 MeV (13.1%), 5.39 MeV (1.6%), 5.54 MeV (0.3%), and 5.51 MeV (0.2%), with a weighted energy average of 5.46 MeV. The nuclide also emits several gamma rays, *e.g.* 59.5 keV (35.9%), enabling activity-calibration measurements using high-purity germanium (HPGe) detectors.

The rather compact design of our alpha-particle irradiator makes it easy to move between different locations. It also makes it possible to perform irradiation experiments under, for example, different temperatures by placing it in an incubator or refrigerator during the irradiation of cells. That latter is important if studies of the temperature dependence of high-LET irradiations are to be performed, investigating bystander signalling or DNA repair under such conditions. Examples of other alpha-particle irradiators that have been constructed earlier include the bench-top system developed in J. Little's laboratory at the Harvard School of Public Health and the system built in R. W. Howell's laboratory at the New Jersey Medical School (17) (18). A bench-top alpha-particle irradiator was also presented at the Massachusetts Institute of Technology by Wang (19).

To investigate the inherent radiation sensitivity of cells exposed to alpha particles, we irradiated six different types of cancer cells using the above mentioned ^{241}Am source and compared the effect with gamma radiation from a standardized ^{137}Cs source. The cells used in this study were three types of prostate cancer and three types of pancreatic cancer cells, *i.e.* LNCaP, DU145, PC3, Capan-1, Panc-1, and BxPC-3. The results can be used in estimating the potential use of TAT against these different types of cancer. Since the developed alpha-particle irradiator also can be used for two-compartment systems, studies are now on-going investigating the bystander effect of alpha particles compared to other types of radiation, such as gamma rays, beta particles, and Auger electrons.

MATERIAL AND METHODS

Below is described how the ^{241}Am source was designed, constructed and calibrated, how the absorbed-dose calculations were performed by MC simulations, and how the cancer cells were grown, irradiated, and evaluated for radiation sensitivity.

Americium-241 Alpha-Particle Source

A custom-made alpha-particle source was ordered from Eckert & Ziegler Isotope Products GmbH, Braunschweig, Germany (via Gammadata Instrument AB, Uppsala, Sweden). The source was produced under ISO standards 2768-m/8769/2919 by electroplating $^{241}AmO_2$ onto an aluminum backing to a final effective circular source size of 11.8 mm in diameter. The activity of the source was determined via a reference measurement using an HPGe-detector and a small (Ø = 2 mm) calibration source of ^{241}Am. The distance from the detector was 60 cm and 10,000 pulses were recorded in the 59.5 keV gamma peak. The alpha-particle energy spectra of the source was measured via Passivated Implanted Planar Silicon (PIPS®)-detector measurements, see below.

The uniformity of the source was estimated by utilizing the emitted 59.5 keV gamma rays and measuring the variation of the optical density on a Gafchromic EBT3 film (ISP, Wayne, New Jersey, USA). The uniformity was determined to vary with ±3.5% across 1000 pixels, equal to the diameter of the source. The alpha-particle energy emitted from ^{241}Am is approximately 5.46 MeV. However, since the alpha particles emitted from the source will have had some of their energy absorbed before leaving the source a measurement of the emitted alpha-particle spectrum was performed using the PIPS® detector. The MC model of the americium source was validated against the measured energy spectrum.

Semiconductor Detector Measurement of the ^{241}Am Source

The ^{241}Am source was measured in vacuum using a PIPS® detector of type A300-17AB (Canberra, Meriden, USA). The electronics used was a preamplifier of type 2003BT (Canberra, Meriden, USA), a voltage supply of type 710 (Canberra, Meriden, USA) and an all-in-one amplifier/ADC/MCA of type DigiDART (EG & ORTEC, Oak Ridge, USA). The DigiDART was used due to its ability to handle high pulse rates with low dead-time. The distance between the ^{241}Am source and the detector surface was set to 36 mm. The measurement time was 180 s and the energy calibration of the system was done using a calibration source electroplated with ^{242}Pu and ^{243}Am.

Defining the ^{241}Am Source and Simulations of the PIPS® Detector using MC

The MC simulations were done using GATE v7.0 (GEANT4 Application for Tomographic Emission) using the GEANT4 version 9.6 patch 03 libraries with the QBBC_EMY physics list (20) (21). GATE, which uses the GEANT4 physics libraries for all simulations, was developed especially for MC simulations of medical imaging and radiotherapy.

All detailed information needed for defining the ^{241}Am source in the MC model could not be provided by the manufacturer. Therefore, the energy spectrum was first measured using the PIPS® detector as described above. In the MC model, the source was then defined using the available information from the manufacturer, which was further modified until the simulations produced an energy spectrum equivalent to the measured energy spectrum.

The minimum thickness of active area in a PIPS® detector is greater than 140 µm, which is sufficient for full-energy absorptions of alpha particles up to 15 MeV. Therefore, the detector and its response were not modeled in the simulations. Instead, the position of the active area, if the PIPS® detector had been included in the simulations, were defined in vacuum. The simulations scored, using GATE's phase space actor, the alpha particles reaching the position of the active area facing the ^{241}Am source. The output from the simulations were further analysed in MATLAB™ (MATLAB Release 2012b, The MathWorks Inc., Natick, MA, USA). Events occurring before the alpha particles reach the active volume, *i.e.* passing the detector window, results in a decrease of spectrum resolution. This was accounted for by broadening the energy spectrum of the scored alpha particles using a Gaussian broadening function with width FWHM/2.335, FWHM = 17 keV (22).

In the simulations, the geometry of the ^{241}Am source included the ^{241}Am source itself and a 0.5 µm thick palladium (12.023 g/cm^3) coating. The silver foil, epoxy and engraving were not included since no exact details about those parameters were available from the manufacturer of the source. The americium layer was modeled as a solid cylinder of AmO_2 (11.68 g/cm^3), with diameter 11.8 mm and height 0.296 mm. The measured energy spectrum, using the PIPS® detector, showed a single broad alpha-particle peak that could not be explained by the detector energy resolution alone. Therefore, it was assumed that the alpha particles were distributed at different depths in the AmO_2, and hence the difference in energy loss before leaving the source resulted in a broadened energy spectrum. The source term in the simulations were therefore divided into 19 circular planar sources, diameter 11.8 mm, and placed at different depths in the AmO_2. The uppermost plane source was placed directly below the palladium coating and the remaining layers were evenly distributed down in the AmO_2 layer in steps of 0.15 µm. Each planar source emitted 5.46 MeV alpha particles isotropically in the 2π-hemisphere facing the PIPS® detector. In total 10 million alpha particles were simulated and the total intensity of the 19 planar sources was set to unity.

The intensity of each planar source was adapted until the simulated energy spectrum showed a similar broadening as in the measured energy spectrum.

In the simulations, the definition of the ^{241}Am source was simplified. Hence, the activity determined using the HPGe-detector is not applicable for the simulated source. The activity of the simulated source was determined by scaling the simulated energy spectrum for the PIPS® detector; the scaling was made with respect to the peak maximum in the simulated and measured energy spectrum, respectively. The scaling factor gave the measurement time represented by a simulation of 10 million alpha particles, which also gave the total activity of the simulated source.

Irradiation Set-Up

Figure 1 shows a drawing of the irradiation set-up. An image of the complete geometry is shown in Figure 2. The ^{241}Am source was placed in an aluminum holder and covered with a 1 µm protective Mylar® film. Well inserts were placed on top of this film, centered at the source. In the well inserts, cells were grown as monolayers on a 10 µm thick polyester membrane at the bottom of the wells. An acrylic glass lid was placed on top of the well inserts to keep them stable during irradiation.

MC Simulations of Absorbed Dose to Cancer Cells

The definition of the ^{241}Am source is described above. The 1 µm thick Mylar® (a polyester film) and the 10 µm thick polyester membrane (1.38 g/cm^3, $C_{10}H_8O_4$) were placed directly on top of the ^{241}Am source. Both layers were modeled as cylinders with radius 5.9 mm and 3.3 mm, respectively, centred above the source. The well inserts, placed directly on top of the polyester layer, were modeled as a polystyrene tube (1.0 g/cm^3, C_8H_8) with wall thickness 1 mm and inner radius 3.2 mm. The cell layer, inside the well inserts, were defined as a water filled cylinder with height 20 µm and radius 3.2 mm. The height was determined after estimations of the diameter of the cell nuclei for the different cancer cells, which was found to be in the range of 18 to 22 µm. Hence, 20 µm was used for all computations for all cell lines. The cell layer was placed directly on top of the polyester layer. The cell-culture medium was defined as a water-filled cylinder placed directly on top of the cell layer, height 4.98 mm and radius 3.2 mm.

The absorbed dose to the cell layer was simulated for 10 million emitted alpha particles. The energy deposition in the cell layer was scored using GATE's sensitive detector, which gives the energy deposition per particle. The absorbed dose was calculated by dividing the sum of all energy depositions with the mass of the cell layer. The energy of the alpha particles entering the cell layer was scored using the phase-space actor. For 2 million simulated alpha particles, the energy of the alpha particles entering the Mylar® layer (*i.e.* the alpha particles leaving the source) was scored using the phase-space actor. Using the SRIM/TRIM software package (which is based on the work on range algorithms by J. P. Biersack) developed by J. Ziegler in the early 80's, the LET spectrum of the alpha particles hitting the cell layer was calculated (23) (24).

Cancer Cells

The prostate cancer-cell lines LNCaP, DU145, and PC3 were purchased from the American Type Culture Collection (ATCC®, Manassas, VA, USA) and grown in Roswell Park Memorial Institute (RPMI) 1640 medium, Eagle's Minimum Essential Medium (EMEM), and Kaighn's Modification of Ham's F-12 (F-12K) medium, respectively, supplemented with 10% fetal

bovine serum (FBS) and 1% penicillin-streptomycin (100 U/mL). The cells were grown in T-75 and/or T-150 flasks as a monolayer and kept at 37 °C in a humidified atmosphere in an incubator at 5% CO_2. Culturing media was changed at least twice per week and the cells passaged before reaching confluence, using trypsin-EDTA. All experiments were carried out with cells in passage-number interval 12−26, 12−23, or 12−22, respectively. The cell-doubling times were determined to be 50, 35, and 30 h for the LNCaP, DU145, and PC3 cells, respectively.

The pancreatic cancer-cell lines Capan-1, Panc-1, and BxPC-3 were purchased from the American Type Culture Collection (ATCC®, Manassas, VA, USA) and grown in Iscove's Modified Dulbecco's Medium (IMDM), Dulbecco's Modified Eagle Medium (DMEM), and Roswell Park Memorial Institute (RPMI) 1640 medium, respectively, supplemented with 10% FBS and 1% penicillin-streptomycin (100 U/mL). The cells were grown as described above. The cells were passaged before reaching confluence using TrypLE™ Select (10X) or TrypLE™ Select (1X). All experiments were carried out with cells not exceeding passage number 14, 20, or 28, respectively. The cell-doubling times were determined to 41, 52, and 48−60 h for the Capan-1, Panc-1, and BxPC-3 cells, respectively.

The cell counting was performed using the The Countess™ automated cell counter that utilizes trypan-blue staining and image-analysis algorithms to identify the total number of cells and the fraction of viable cells (Life Technologies Ltd., Paisley, UK).

^{241}Am and ^{137}Cs Irradiations

The LNCaP, DU145, PC3, Capan-1, Panc-1, and BxPC-3 cells were, at each radiation experiment, each seeded into two removable well inserts of a 24-well plate (Thermo Fisher Scientific Inc., MA, USA) at an approximate cell density of 10,000 cells/well in 100 or 200 µL culture medium. Two additional wells were filled with the same amount of medium without any cells present and used as controls. After 2−3 d of recovery, the medium was changed and the cells were irradiated to desired absorbed dose level. Controls were treated in exact same manner, without being irradiated. Before each irradiation, it was confirmed that the cells grew in a monolayer by inspection using a light microscopy. For the alpha-particle irradiations, each removable well-insert was placed on top of the ^{241}Am source in the fixture and geometry as described above and irradiated to desired absorbed dose. For each new irradiation the sterilized Mylar film was replaced in order to minimize the risk of contamination. For the ^{137}Cs irradiations, the well inserts were placed in the ^{137}Cs irradiator Gammacell 40 Exactor (Best Theratronics Ltd., Ashford, UK), and irradiated to desired absorbed dose. The absorbed dose rate during the ^{137}Cs irradiations was 0.86 Gy/min. Regarding ^{137}Cs, some irradiations were also done using 96-well plates, for comparison with those irradiations done using 24-well plates including subsequent transfer to 96-well plates enabling read-out of the surviving fractions.

Radiation Sensitivity Measurements

After irradiation the cells were left in an incubator for a time period equal to the specific cell-doubling time plus at least one day. Each well insert was gently washed with cell media twice and the cells therein were then very carefully trypsinized and transferred to three individual wells on a 96-well plate in 100 or 200 µL of fresh medium, after which the protocol for cell viability measurements was initiated. Cell viability was determined by a tetrazolium salt-based calorimetric assay using the Cell Proliferation Reagent WST (water soluble tetrazolium)-1 kit (Roche Applied Science GmbH, Pensberg, Germany). The WST-1 kit is

especially manufactured for non-radioactive spectrophotometric quantification of, for example, cell viability. The tetrazolium salt in the kit, once added to a cell solution, is reduced to the colored compound formazan by mitochondrial dehydrogenase enzymes and gives a direct correlation to the number of metabolically active or viable cells in the solution. For each 96-plate well, 10% of WST-1 solution was added and incubated for at least 4 h at 37 °C in 5% CO_2 in a humidified atmosphere. The absorbance of the dissolved formazan product was measured at 450 nm on a Labsystems Multiscan Plus plate reader using the DeltaSoft JV software (BioMetallics Inc., Princeton, NJ, USA). The mean value from measurements of fresh medium containing 10% WST-1 was used for absorbance background correction and untreated cells were used as control.

RESULTS

This study shows that it is possible to construct a bench-top easy to use external alpha-particle irradiator for use in radiation sensitivity studies. Once it has been calibrated and the geometry has been fixed it can be used repeatedly with no extra calibration needed, due to the long half-life of ^{241}Am.

The activity of the ^{241}Am source was found to be 405 ± 10 kBq according to the HPGe-detector measurements, which is in good agreement with the PIPS®-detector based MC simulations, which resulted in an estimated total activity of 417 kBq if self-absorptions of the gamma rays emitted from ^{241}Am were taken into account. Figure 3 shows the measured energy spectrum and the simulated energy spectrum for the PIPS® detector. The MC simulated full-energy peak overlaps with this measured full-energy peek completely. Figure 4 shows the energy spectrum of the alpha particles hitting the cell monolayer as calculated by the MC simulations (peak energy = 3.20 MeV), as well as PIPS®-detector measured energy spectrum (peak energy = 4.98 MeV). The figure clearly shows that the processes occurring before the alpha particles reach the cell layer result in a lowering of the mean energy as well as a greater spread in alpha-particle energies. Figure 5 shows the LET spectrum of the alpha particles hitting the monolayer of cells. As mentioned before, Figure 1 and 2 illustrates the geometry and irradiation set-up during the alpha-particle irradiations. The calculated absorbed-dose rate in this set-up and under the declared assumptions stated above was 1.05 Gy/min.

The study also shows that irradiating cancer cells by alpha particles has a significantly more lethal effect than compared to ^{137}Cs irradiations. Especially, the RBE values for the alpha particles, relative to the gamma irradiation from ^{137}Cs at 37% cell survival, for the LNCaP, DU145, PC3, Capan-1, Panc-1, and BxPC-3 cells were 7.9 ± 1.7, 8.0 ± 0.8, 7.0 ± 1.1, 12.5 ± 1.6, 9.4 ± 0.9, and 6.2 ± 0.7, respectively (Table 1, Figure 6a-f). For the alpha-particle irradiations, the survival fractions at 2 Gy (SF2) were 0.03 ± 0.01, 0.02 ± 0.01, 0.02 ± 0.01, < 0.01, 0.01 ± 0.01, and 0.02 ± 0.01, respectively (Table 1, Figure 6a-f). For the gamma irradiations the SF2 values were 0.66 ± 0.12, 0.65 ± 0.05, 0.62 ± 0.10, 0.61 ± 0.08, 0.72 ± 0.16, and 0.62 ± 0.044, respectively (Table 1, Figure 6a-f). The α/ß ratios for the gamma irradiation were 8.7, 14.2, 17.4, 15.7, 5.3, and 17.9, respectively (Table 1, Figure 6a-f).

DISCUSSION

The present study reports on how to construct and calibrate an easy-to-use and relatively low-cost alpha irradiator for establishing a constant broad beam of alpha particles to a monolayer of cells. Also is described how to with Monte Carlo technique an accurate dosimetry can be performed. The intention was to create an irradiation geometry that could be available for radiation-sensitivity experiments at any time. Alpha particles are an important type of radiation to include in such studies, besides the use of gamma rays, beta-, or Auger-electrons. There are three dominant alpha-particle energies emitted from ^{241}Am; 5.48 MeV, 5.44 MeV, and 5.39 MeV. This means that the alpha-particle energy emitted from the source is almost monoenergetic. However, since the beam of alpha particles pass though a Mylar® film and a polystyrene membrane before reaching the cell layer some attenuation of the beam, and hence broadening of the energy spectra, will occur. This is illustrated in Figure 4 and Figure 5, showing the energy and LET spectrum of the alpha particles hitting the cells, respectively. An interesting basic radiobiological experiment would be to irradiate cells with a true mono-energetic alpha-particle beam, and investigating the radiation sensitivity for defined values of LET. However, in a clinical situation the cells will always be hit by alpha particles of a wide range of energies and LET values. And since this is a preclinical study, we think it is valuable to perform the experiments as presented here.

Semiconductor Measurements and MC Simulations

Some modifications of the simulated ^{241}Am source were made in the MC model. The exact thickness of stated epoxy and silver layers by the manufacturer could not be provided, and the stated 2 µm palladium coating was set to 0.5 µm; the manufacturer could not verify the exact thickness and a thicker palladium coating than 0.5 µm resulted in a too high energy loss for the alpha particles. The discrepancies in thickness might be explained by: the coating is thinner than that stated by the manufacturer, the thickness is non-homogenous, or the coating is an alloy of palladium and an additional element not stated by the manufacturer.

The measured energy spectrum in Figure 3, shows a single broad peak. The PIPS® detector has a high-energy resolution (FWHM = 17 keV), and the broad peak must therefore be caused by the source geometry. A homogenous distribution of alpha particles in the AmO_2 layer did not produce a similar broadening, regardless if the energy of the alpha particles were defined as the mean energy or using all alpha particles emitted (and their respective intensities) in a ^{241}Am decay. The shape of the measured energy spectrum suggested that a heterogeneous distribution of alpha particles could create a similar broadening. Therefore, 19 circular planar sources were defined and placed at different depths in the AmO_2 layer. The tail on the left side of the full energy peak in the measured energy spectrum is not seen in the simulated energy spectrum. The tail can be divided into two parts. The first part starts at where the measured values differs from the simulated and ends at ~4.1 MeV. The difference between measurement and simulation can be explained by the following factors in the measurement set-up: a heterogeneous depth distribution of the americium in the source, an uneven detector dead layer, not high enough vacuum reached in the vacuum chamber, and geometrical effects. The americium distribution is most likely the most important factor and in future works, more attention should be given to definition of source in the MC model. The second part of the tail, from ~4.1 MeV to 0 MeV, cannot be explained by the already mention factors. This part of the tail is probably caused by an insufficient piled-up rejection in the detector electronics and electronic noise, both caused by the high count rate. However, the entire left-side tail of the measured spectra in Figure 3

contains only approximately 1 ‰ of the total number of counts, and gives therefore a very limited contribution of the total number of particles, and hence absorbed dose.

Modeling the PIPS® response would require exact knowledge about the detector design (which is not possible) and validation measurements. We believe that the approach used in this work, *i.e.* all alpha particles reaching the active volume deposits their entire energy and the energy straggling is accounted for using the Gaussian broadening function, is a reasonable simplification. The MC model of the source is of course not an exact replica of the real source, and it is therefore not expected that the simulated energy spectrum and activity would exactly match the measured energy spectrum and activity. Though, a large deviation between simulations and measurements would imply that the MC model is not sufficient. Since there is a good agreement between simulated and measured activity as well as between simulated and measured energy spectrum, it can be assumed that the MC model gives a good estimation of the absorbed dose, given that the cells can be modeled as a homogenous water layer with a thickness of 20 µm.

Another possibility of modeling the alpha-particle source is to use a measured energy spectrum as the definition of a source spectrum in the simulations. The angular distribution, and hence the energy of the alpha particles, reaching the detector volume changes with source-detector distance. The PIPS® detector would therefore had to be placed at the same position as the cell layer, which however was not possible in this study due to high dead times.

Absorbed Dose to Cancer Cells

Calculating the absorbed dose from the alpha particles as a mean dose, especially when considering low absorbed doses, can induce statistical uncertainties. Depending on initial alpha-particle energy, where on the Bragg curve the alpha particle is when it enters the cell, and how large the cell nucleus is, the energy imparted by a single alpha-particle traversal through a cell nucleus differs, but could be in the order of 0.2 Gy. And, the statistical uncertainty at low absorbed doses could be considerable with respect to how large fraction of the cells have received for example 0, 1, 2, or 3 hits by alpha particles. Such situations could in some cases be dealt with using microdosimetry (25). However, in order to have complete control over the statistics microbeam studies have to be performed, in which full control over which cells have received hits and how many hits they have received is made possible (26). Such studies are possible only at a handful research fascilities around the world. We are now planning for both a microdosimetric analysis of the irradiation set-up presented in this paper, as well as for microbeam experiments for some of the cell lines studied here. Contribution of gamma radiation from ^{241}Am to the absorbed dose to the cells was in the order of 10^{-5} to that from the alpha particles, and could therefore be ignored.

Radiation Sensitivity Measurements

Regarding the radiation-sensitivity measurements, using the WST-1 assay has some advantages, but also some drawbacks. On the positive side, it is easy to use, it is possible to repeat measurements on the same well insert several times without killing the cells, and it gives a result regarding the radiation sensitivity fairly quickly, with a limited amount of work. We also believe that it is more operator independent than, for example, the colony-forming assay. On the negative side, the WST-1 assay is not as sensitive as the colony-forming assay for high absorbed doses, *i.e.* small surviving fractions under one percent. This applies to all tetrazolium-based assays (*e.g.* the MTT assay) in comparison to colony forming. It has

previously been shown that tetrazolium-based assays to some degree overestimate the surviving fraction for absorbed doses over approximately 8−10 Gy (27). But since we limited this study to maximum 10 Gy and also used the WST-1 assay for all our evaluations, we believe that the comparison of the effects of gamma and alpha-particle irradiations are comparable. It is also important to have control of the cell number and time of measurement when using a tetrazolium-based method (28). In this study, where the absorbed doses for several cell lines were examined, we chose the WST-1 assay instead of colony forming because it was relatively easy to use and also more operator independent. By using a tetrazolium assay, it was possible to obtain survival-fraction data for large sample throughput in less time, and with less effort, compared to a colony-forming assay.

Repair of Double Strand Breaks

Regarding the results of the inherent radiation sensitivity and levels of surviving fractions for different levels of absorbed dose, it is interesting that the cells' ability to deal with the damages caused by the alpha particles seem to differ to some degree between the cell lines used in this study (Figure 6a-f). When alpha particles pass through a cell, double strand breaks (DSBs) in the cell's nucleus are supposed to be the major cause to cell death. The two major mechanisms by which mammalian cells are able to repair such DSBs are via homologous recombination (HR) or non-homologous end-joining (NHEJ). A deficiency in promoting HR and/or NHEJ would mean a decreased ability to deal with DSBs. In this study DU145, Capan-1, and Panc-1 were the least radioresistant cells when exposed to alpha particles, with RBEs (and coefficients in the mono-exponential equations in parenthesis) equal to 8.0 ± 0.8 (-1.864), 12.5 ± 1.6 (-2.968), and 9.4 ± 0.9 (-2.006), respectively. For at least one of the cell lines (Capan-1), a plausible explanation for this is that a mutation in BRCA2 influences the cells ability to promote HR (29). At the same time, BRCA2 promotes the HR pathway (via the effector protein Rad51) but have no impact on NHEJ (unlike BRCA1 which is involved in both the HR and NHEJ pathways), and has also been shown to be mutated in approximately 10% of pancreatic cancers (30). And, regarding prostate cancer mutations in BRCA2, it has previously been shown to be present, as well as influencing early-onset prostate cancer (31) (32) (33). An interesting follow-up study would be to quantify the level of mutations in BRCA2 in the cell lines used in this paper, and to correlate the level of mutation with the cell lines' sensitivity to alpha-particle irradiation.

CONCLUSIONS

This study shows that it is possible to construct a bench-top, easy to use, external alpha-particle irradiator for use in radiation-sensitivity experiments. Once calibrated the alpha-particle irradiator can be used repeatedly with no extra calibration needed, due to the long half-life of ^{241}Am. And, dosimetry can performed with MC simulations. The results clearly show that irradiating cancer cells by alpha particles has a significantly more lethal effect than compared to ^{137}Cs irradiations. Especially, Capan-1 cells shows a particularly high sensitivity for alpha-particle irradiation, with an RBE = 12.5 and a coefficient in the mono-exponential function describing the effect of this type of radiation equal to 2.97. Although it is difficult to draw any conclusions regarding the α/β ratio in the bi-exponential curve fit for the ^{137}Cs irradiations and compare with clinical values defining early and late responding tumor tissues, we still believe it is valuable to state these ratios as a comparison between the cells in this study.

There are always uncertainties accompanied with this kind of studies. With respect to uncertainties in the measured exposure time during the alpha-particle irradiations, estimations of the diameter of the cell nucleuses, fluctuations in the uniformity of the alpha-particle source, we estimate the calculated absorbed dose vary at maximum as ±10% from a true value. And hence, we believe the conclusions drawn from the experiments are still valid under the circumstances stated. The overall results indicate that both prostate and pancreatic cancer are very good candidates for further studies of RIT using specific mAbs labeled with relevant alpha-particle emitters. Interesting potential up-coming studies includes investigating the role of BRCA2 for HR after alpha-particle exposure, and also performing microbeam studies for the cell lines investigated here.

ACKNOWLEDGMENTS

Crister Ceberg is acknowledged for help with the dosimetry film during the uniformity measurements of the ^{241}Am source. Erik Larsson is acknowledged for help during the HPGe measurements of the source. The fixture and source holder were skillfully constructed by Sven Brink. This study was performed with generous support from the Swedish Cancer Foundation, Mrs. Berta Kamprad's Foundation, and Gunnar Nilsson's Foundation.

REFERENCES

1. Becquerel H. Sur les radiations invisibles émises par les corps phosphorescents. Comptes Rendus 1896:420.

2. Rutherford E. Uranium radiation and the electrical conduction produced by it. Philosophical Magazine 1899;5:109.

3. Elgqvist J, Frost S, Pouget JP, et al. The potential and hurdles of targeted alpha therapy - clinical trials and beyond. Front Oncol 2014;3:324.

4. Kim YS, Brechbiel MW. An overview of targeted alpha therapy. Tumour Biol 2012;33:573.

5. Allen BJ. Future prospects for targeted alpha therapy. Curr Radiopharm 2011;4:336.

6. Sgouros G. Alpha-particles for targeted therapy. Adv Drug Deliv Rev 2008;60:1402.

7. Zalutsky MR. Targeted alpha-particle therapy of microscopic disease: Providing a further rationale for clinical investigation. J Nucl Med 2006;47:1238.

8. Vaidyanathan G, Zalutsky MR. Targeted therapy using alpha emitters. Phys Med Biol 1996;41:1915.

9. Sgouros G, Roeske JC, McDevitt MR, et al. MIRD Pamphlet No. 22 (abridged): radiobiology and dosimetry of alpha-particle emitters for targeted radionuclide therapy. J Nucl Med 2010;51:311.

10. ICRU Report 16. Linear energy transfer. International Comission on Radiation Units and Measurements 1970;16:1.

11. Humm JL, Howell RW, Rao DV. Dosimetry of Auger-electron-emitting radionuclides: report no. 3 of AAPM Nuclear Medicine Task Group No. 6. Med Phys 1994;21:1901.

12. Wiseman GA, White CA, Witzig TE, et al. Radioimmunotherapy of relapsed non-Hodgkin's lymphoma with zevalin, a 90Y-labeled anti-CD20 monoclonal antibody. Clin Cancer Res 1999;5:3281.

13. Chinn PC, Leonard JE, Rosenberg J, et al. Preclinical evaluation of 90Y-labeled anti-CD20 monoclonal antibody for treatment of non-Hodgkin's lymphoma. Int J Oncol 1999;15:1017.

14. Goldsmith SJ. Radioimmunotherapy of lymphoma: Bexxar and Zevalin. Semin Nucl Med 2010;40:122.

15. Rutar FJ, Augustine SC, Kaminski MS, et al. Feasibility and safety of outpatient Bexxar therapy (tositumomab and iodine I 131 tositumomab) for non-Hodgkin's lymphoma based on radiation doses to family members. Clin Lymphoma 2001;2:164.

16. Radium - 223 (Xofigo) for prostate cancer. Med Lett Drugs Ther 2013;55:79.

17. Metting NF, Koehler AM, Nagasawa H, et al. Design of a benchtop alpha particle irradiator. Health physics 1995;68:710.

18. Neti PV, de Toledo SM, Perumal V, et al. A multi-port low-fluence alpha-particle irradiator: fabrication, testing and benchmark radiobiological studies. Radiat Res 2004;161:732.

19. Wang R. Direct and indirect effects of alpha-particle irradiations of human prostate tumor cells. PhD Thesis, Masschusetts Institute of Technology. 2005.

20. Jan S, Santin G, Strul D, et al. GATE: a simulation toolkit for PET and SPECT. Phys Med Biol 2004;49:4543.

21. Amako K, Apostolakis J, Araujo H, et al. Geant4 developments and applications. IEEE Transactions on Nuclear Science 2006;53:270.

22. Canberra Industries Inc. Passivated implanted planar silicon (PIPS®) detectors. www.canberra.com. Data sheet number C39313-04/12. 2012.

23. Biersack JP, Haggmark LG. A Monte Carlo computer program for the transport of energetic ions in amorphous targets. Nucl Instr Meth 1980;174:257.

24. Ziegler JF, Biersack JP, Littmark U. The stopping and range of ions in matter. Pergamon 1985.

25. ICRU Report 36. Microdosimetry. International Comission on Radiation Units and Measurements 1985.

26. Proceedings of the 8th international workshop: Microbeam probes of cellular radiation response. Radiat Res 2009;50:81.

27. Buch K, Peters T, Nawroth T, et al. Determination of cell survival after irradiation via clonogenic assay versus multiple MTT Assay--a comparative study. Radiat Oncol 2012;7:1.

28. Price P, McMillan TJ. Use of the tetrazolium assay in measuring the response of human tumor cells to ionizing radiation. Cancer Res 1990;50:1392.

29. Xia F, Taghian DG, DeFrank JS, et al. Deficiency of human BRCA2 leads to impaired homologous recombination but maintains normal nonhomologous end joining. Proceedings of the National Academy of Sciences of the United States of America 2001;98:8644.

30. Goggins M, Schutte M, Lu J, et al. Germline BRCA2 gene mutations in patients with apparently sporadic pancreatic carcinomas. Cancer Res 1996;56:5360.

31. Agalliu I, Karlins E, Kwon EM, et al. Rare germline mutations in the BRCA2 gene are associated with early-onset prostate cancer. Br J Cancer 2007;97:826.

32. Edwards SM, Kote-Jarai Z, Meitz J, et al. Two percent of men with early-onset prostate cancer harbor germline mutations in the BRCA2 gene. Am J Hum Genet 2003;72:1.

33. Gayther SA, de Foy KA, Harrington P, et al. The frequency of germ-line mutations in the breast cancer predisposition genes BRCA1 and BRCA2 in familial prostate cancer. The Cancer Research Campaign/British Prostate Group United Kingdom Familial Prostate Cancer Study Collaborators. Cancer Res 2000;60:4513.

FIGURE LEGEND

Figure 1. Geometry of the ^{241}Am alpha-particle irradiator showing the: well insert (**A**); cell media (**B**); monolayer of cancer cells (**C**); circular polyester bottom of the well insert (10 µm thick and 6.5 mm in diameter) (**D**); the 1 µm thick Mylar® film (**E**); disk shaped palladium coated ^{241}Am source (0.3 mm thick 11.8 mm in diameter) (**F**); and aluminum backing (height = 5 mm, diameter = 25 mm) (**G**).

Figure 2. Picture showing the set-up during the alpha-particle irradiations. Shown is the fixture holding the well insert at place during irradiation (**A**); the well insert containing cell media and the monolayer of cells at the bottom (**B**); a sterilized Mylar® film (**C**); the ^{241}Am source in a circular aluminum backing (**D**), and the aluminum source holder (**E**).

Figure 3. PIPS®-detector measured alpha-particle energy spectrum from the ^{241}Am source in logarithmic scale with peak energy of 4.98 MeV (○). Shown is also the Monte Carlo simulated PIPS®-detector response (■).The full-energy peak of the measured and the simulated energy spectrum, respectively, overlaps completely.

Figure 4. Normalized energy spectra. The Monte Carlo simulated energy spectrum of alpha particles hitting the cell monolayer (■), with peak maximum energy at 3.20 MeV. The PIPS®-detector measured energy spectrum (○), with peak maximum energy of 4.98 MeV.

Figure 5. Alpha-particle LET spectrum of particles hitting the cell monolayer as calculated by the SRIM/TRIM software package. The peak LET being 124.3 keV/µm.

Figure 6a. Surviving fraction (SF) as a function of absorbed dose (D) for alpha particles from ^{241}Am (■) and gamma rays from ^{137}Cs (▲) for **LNCaP** cells. Shown data points are mean ± SD. Solid line: curve fitting according to the given equation in figure. Dash-dotted line: 95% confidence bands for the curve fitting.

Figure 6b. SF as a function of absorbed dose (D) for alpha particles from ^{241}Am (■) and gamma rays from ^{137}Cs (▲) for **DU145** cells. Shown data points are mean ± SD. Solid line: curve fitting according to the given equation in figure. Dash-dotted line: 95% confidence bands for the curve fitting.

Figure 6c. SF as a function of absorbed dose (D) for alpha particles from ^{241}Am (■) and gamma rays from ^{137}Cs (▲) for **PC3** cells. Shown data points are mean ± SD. Solid line: curve fitting according to the given equation in figure. Dash-dotted line: 95% confidence bands for the curve fitting.

Figure 6d. SF as a function of absorbed dose (D) for alpha particles from ^{241}Am (■) and gamma rays from ^{137}Cs (▲) for **Capan-1** cells. Shown data points are mean ± SD. Solid line: curve fitting according to the given equation in figure. Dash-dotted line: 95% confidence bands for the curve fitting.

Figure 6e. SF as a function of absorbed dose (D) for alpha particles from ^{241}Am (■) and gamma rays from ^{137}Cs (▲) for **Panc-1** cells. Shown data points are mean ± SD. Solid line:

curve fitting according to the given equation in figure. Dash-dotted line: 95% confidence bands for the curve fitting.

Figure 6f. SF as a function of absorbed dose (D) for alpha particles from ^{241}Am (■) and gamma rays from ^{137}Cs (▲) for **BxPC-3** cells. Shown data points are mean ± SD. Solid line: curve fitting according to the given equation in figure. Dash-dotted line: 95% confidence bands for the curve fitting.

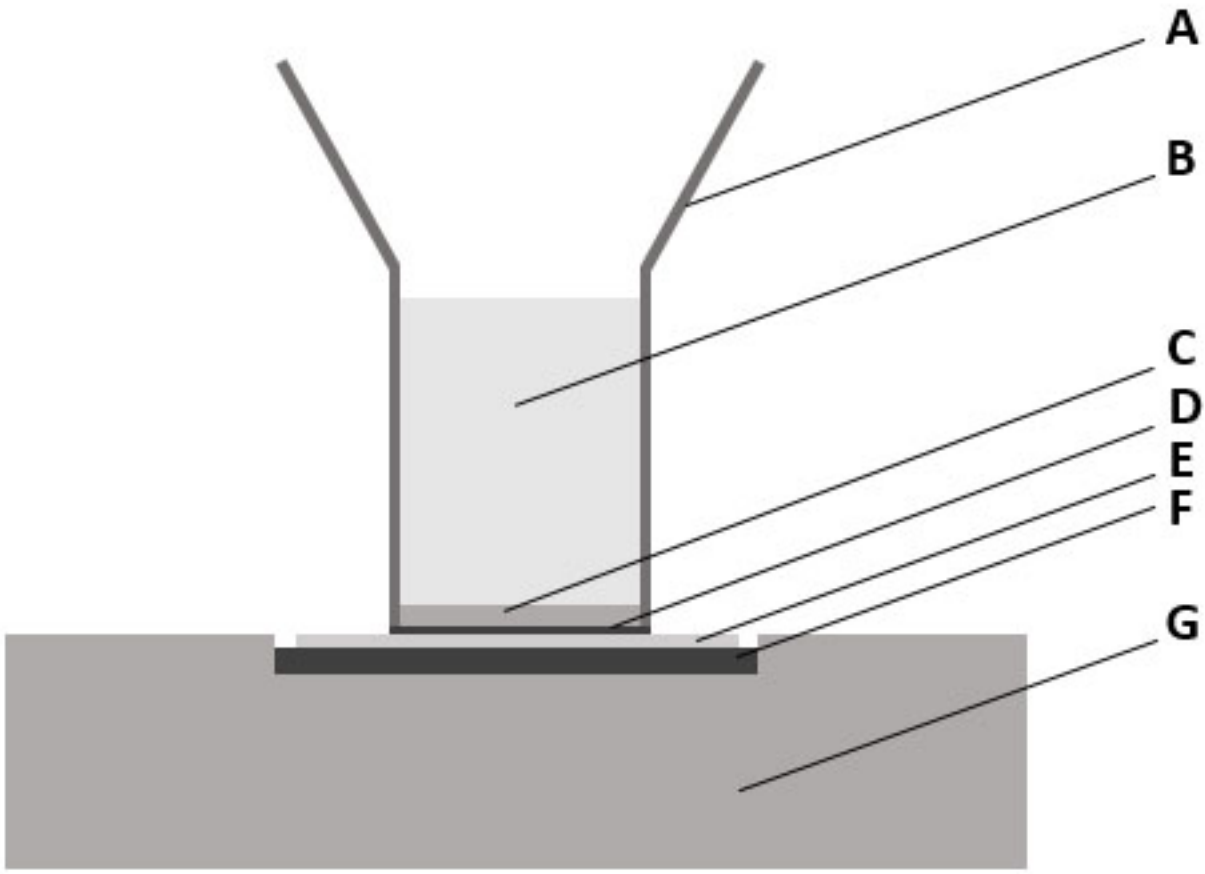
A
B
C
D
E
F
G

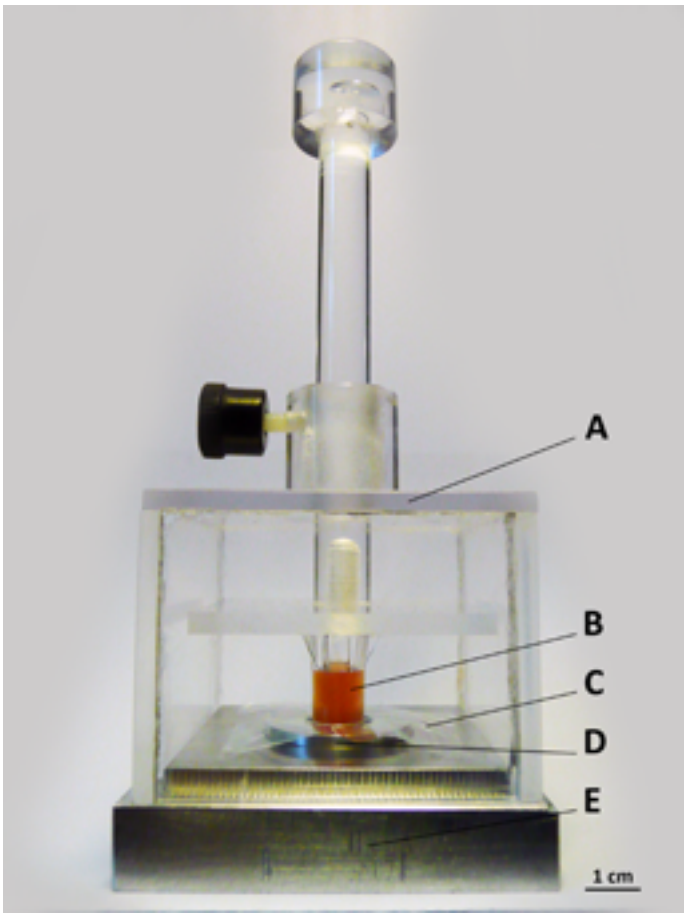
A
B
C
D
E
1 cm

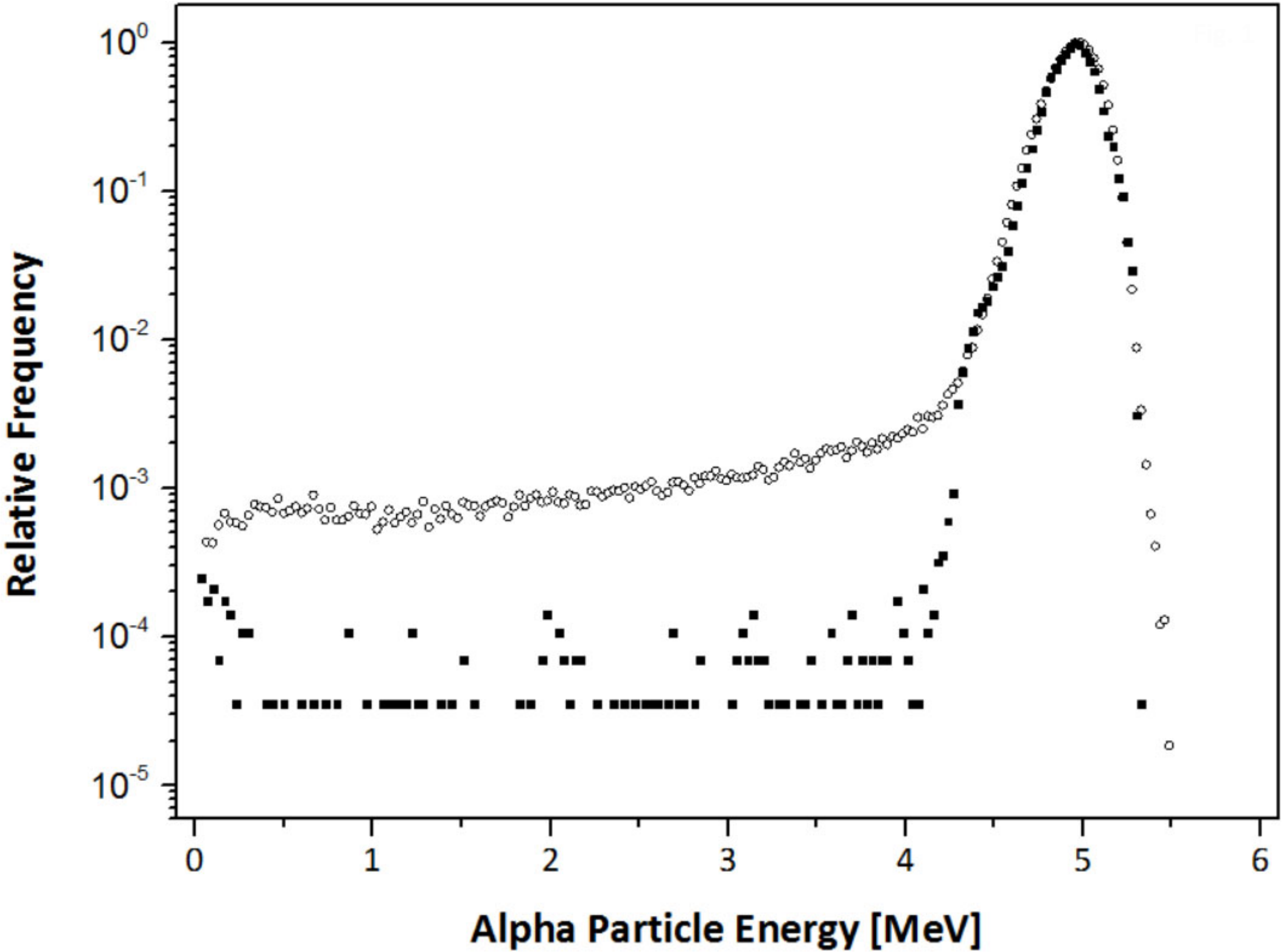
Relative Frequency
10^{0}
10^{-1}
10^{-2}
10^{-3}
10^{-4}
10^{-5}
0
1
2
3
4
5
6
Alpha Particle Energy [MeV]

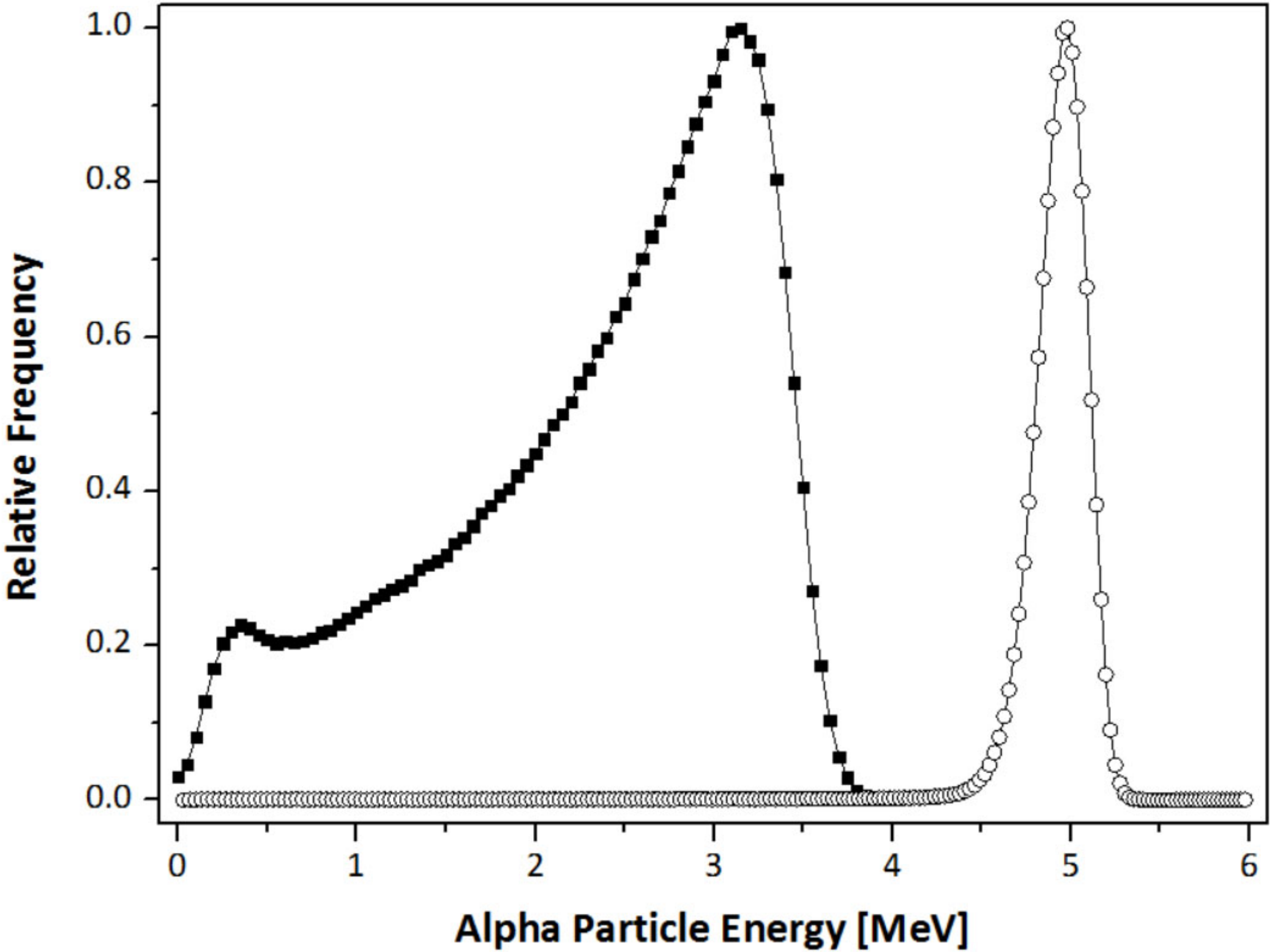
Relative Frequency
1.0
0.8
0.6
0.4
0.2
0.0
0
1
2
3
4
5
6
Alpha Particle Energy [MeV]

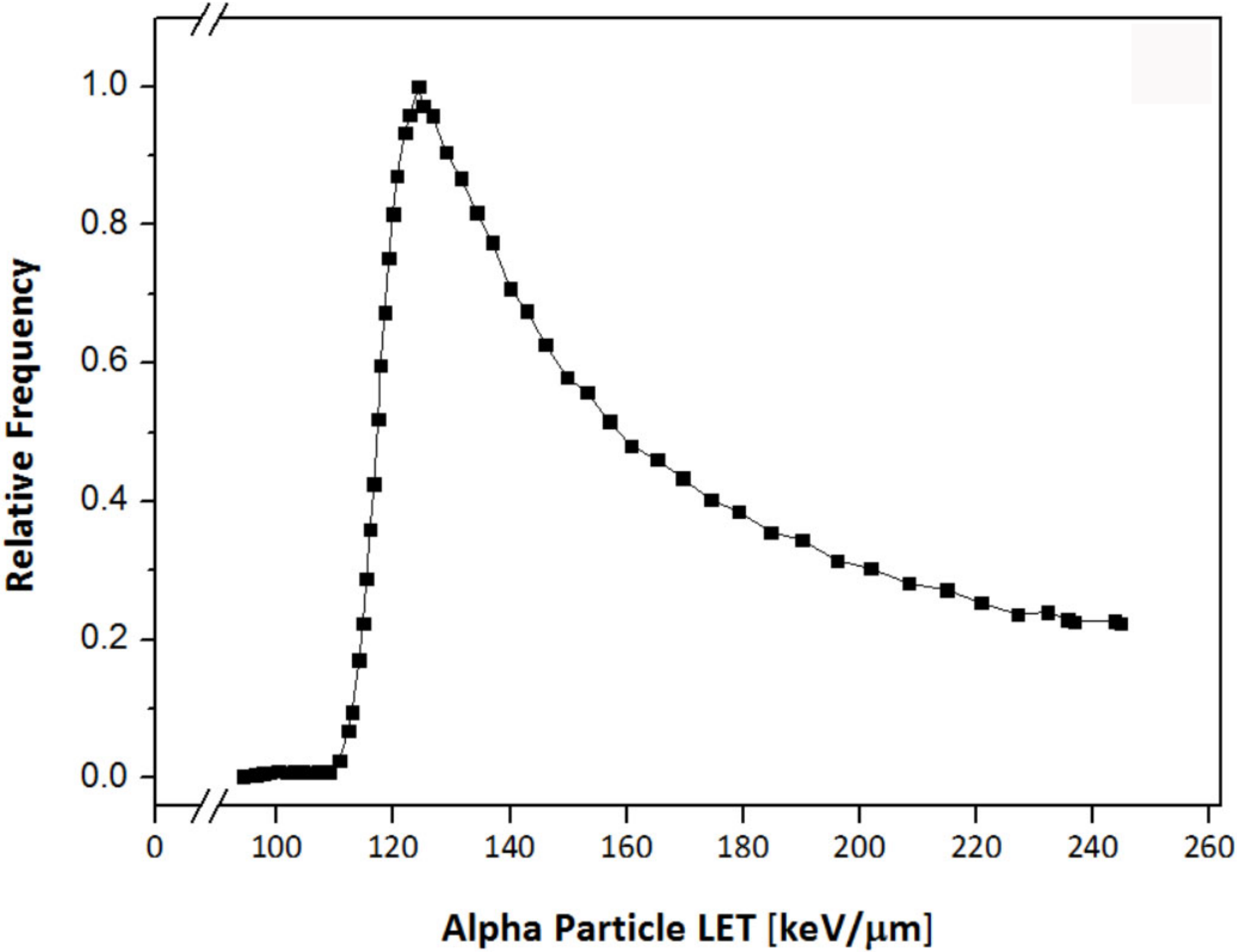
Relative Frequency
1.0
0.8
0.6
0.4
0.2
0.0
0
100
120
140
160
180
200
220
240
260
Alpha Particle LET [keV/µm]

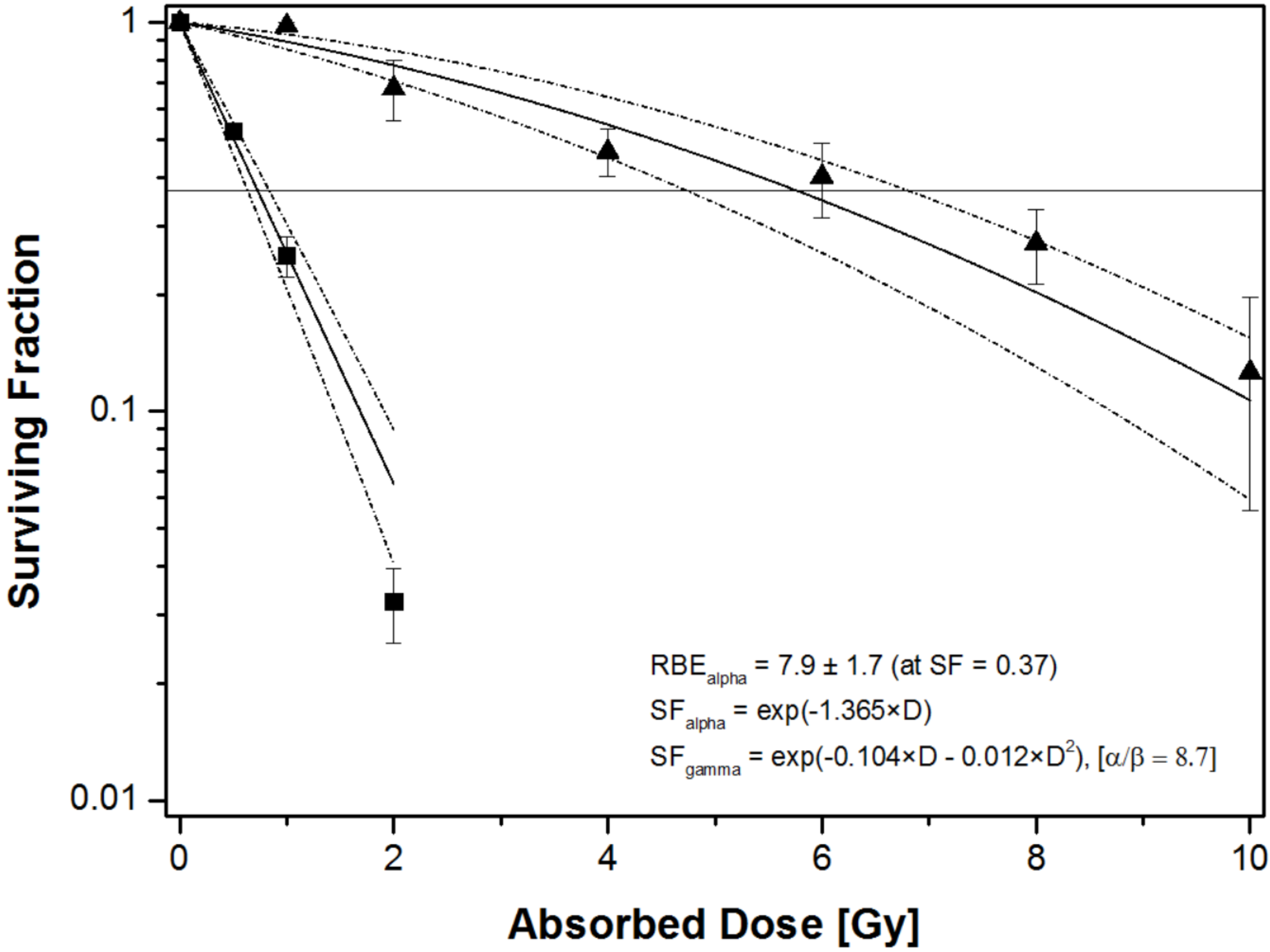
Surviving Fraction
1
0.1
0.01
0
2
4
6
8
10
Absorbed Dose [Gy]
RBE$_{alpha}$ = 7.9 ± 1.7 (at SF = 0.37)
SF$_{alpha}$ = exp(-1.365×D)
SF$_{gamma}$ = exp(-0.104×D - 0.012×D^2), [$\alpha/\beta = 8.7$]

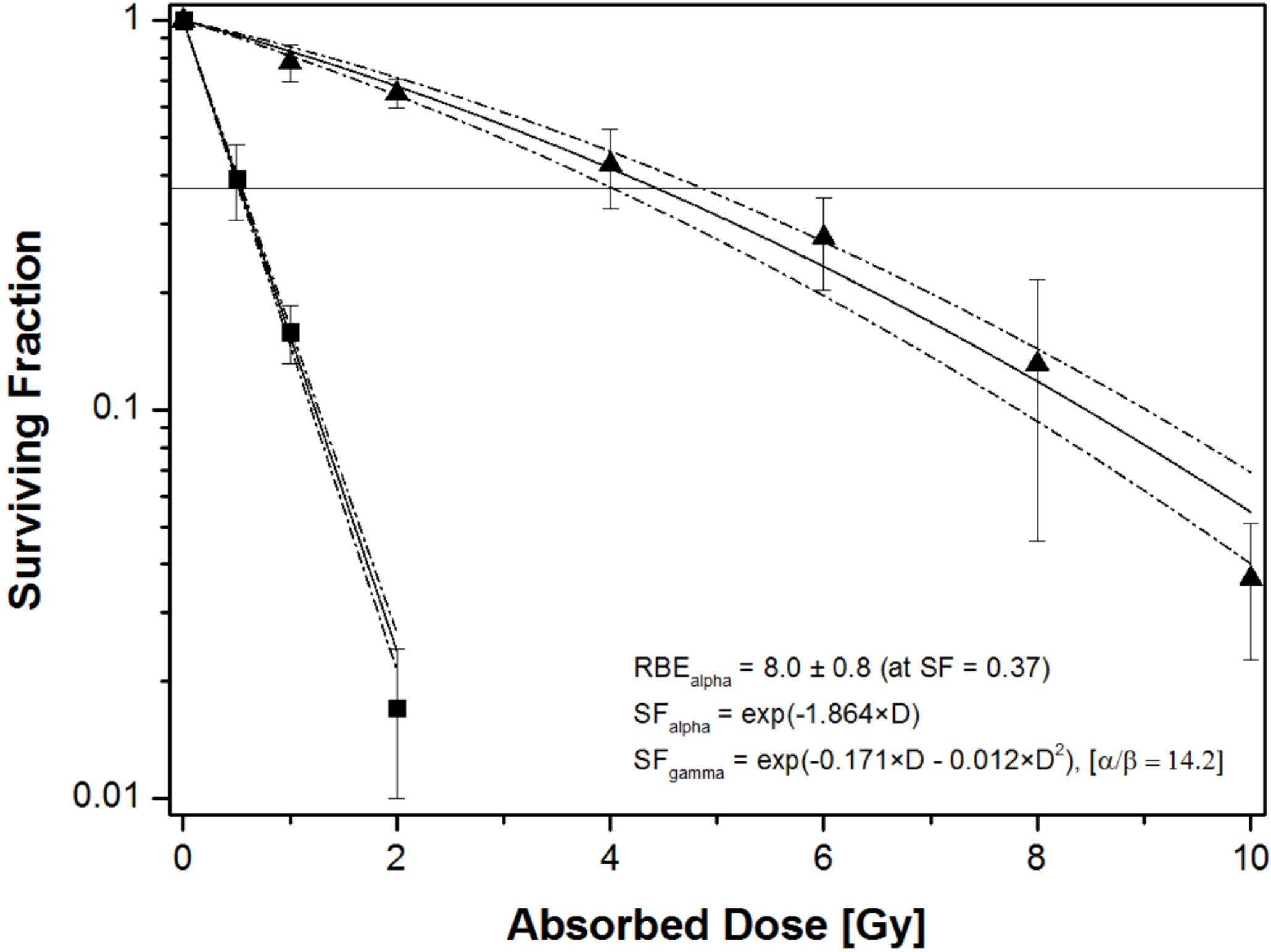
Surviving Fraction
1
0.1
0.01
0
2
4
6
8
10
Absorbed Dose [Gy]
RBE$_{alpha}$ = 8.0 ± 0.8 (at SF = 0.37)
SF$_{alpha}$ = exp(-1.864×D)
SF$_{gamma}$ = exp(-0.171×D - 0.012×D^2), [$\alpha/\beta = 14.2$]

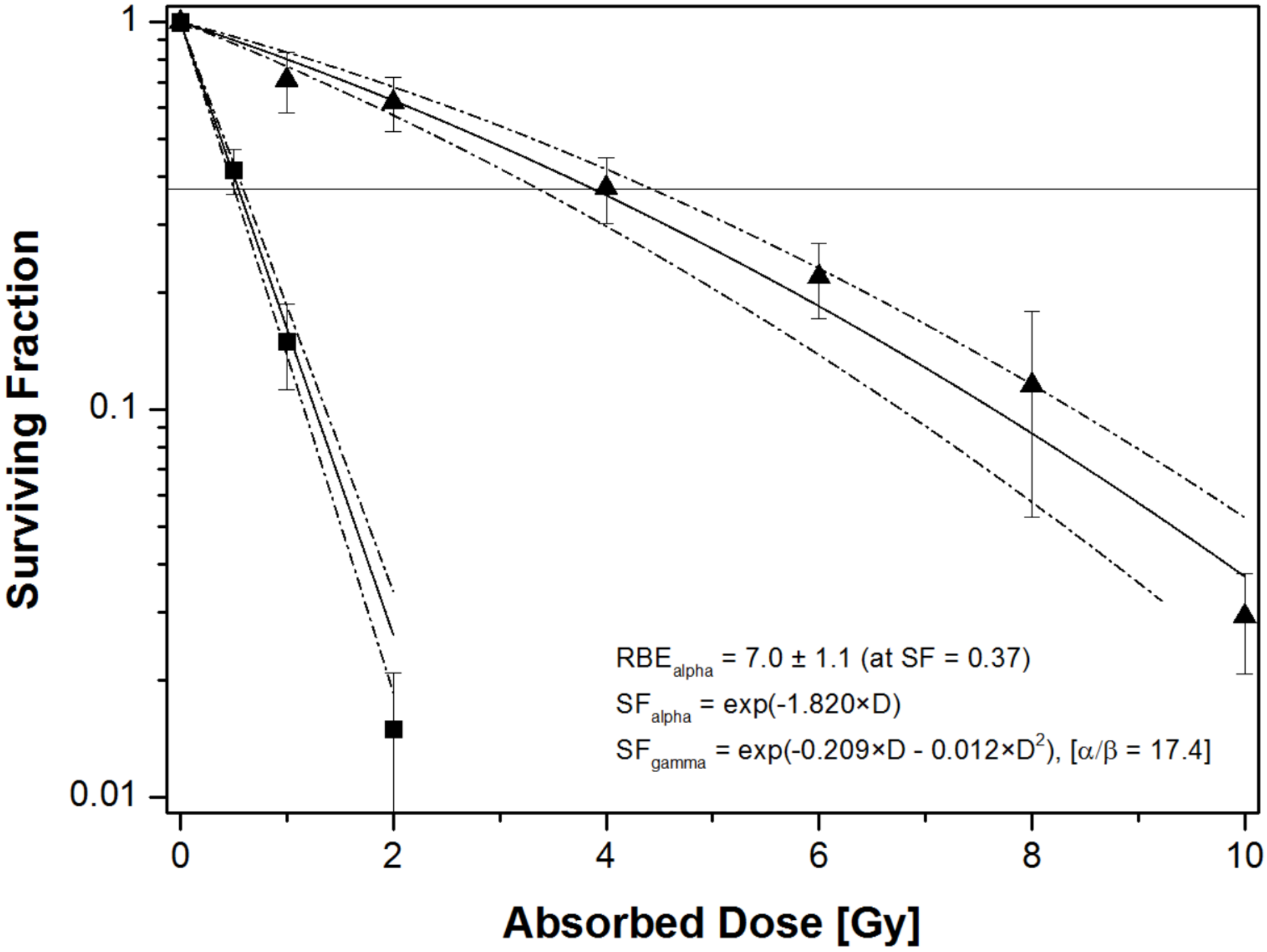
Surviving Fraction
1
0.1
0.01
0
2
4
6
8
10
Absorbed Dose [Gy]
RBE$_{alpha}$ = 7.0 ± 1.1 (at SF = 0.37)
SF$_{alpha}$ = exp(-1.820×D)
SF$_{gamma}$ = exp(-0.209×D - 0.012×D^2), [α/β = 17.4]

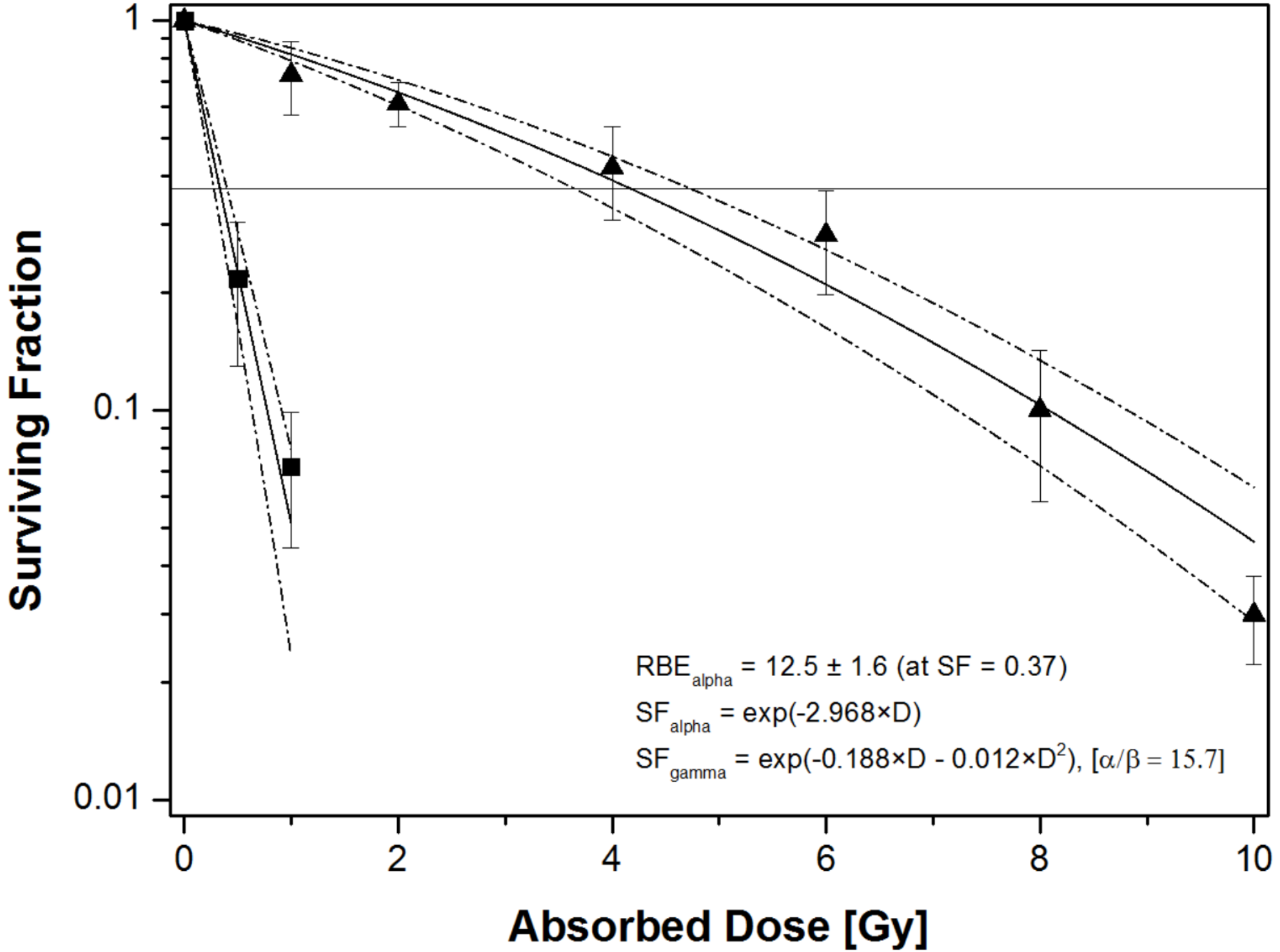
Surviving Fraction
1
0.1
0.01
0
2
4
6
8
10
Absorbed Dose [Gy]
RBE$_{alpha}$ = 12.5 ± 1.6 (at SF = 0.37)
SF$_{alpha}$ = exp(-2.968×D)
SF$_{gamma}$ = exp(-0.188×D - 0.012×D^2), [α/β = 15.7]

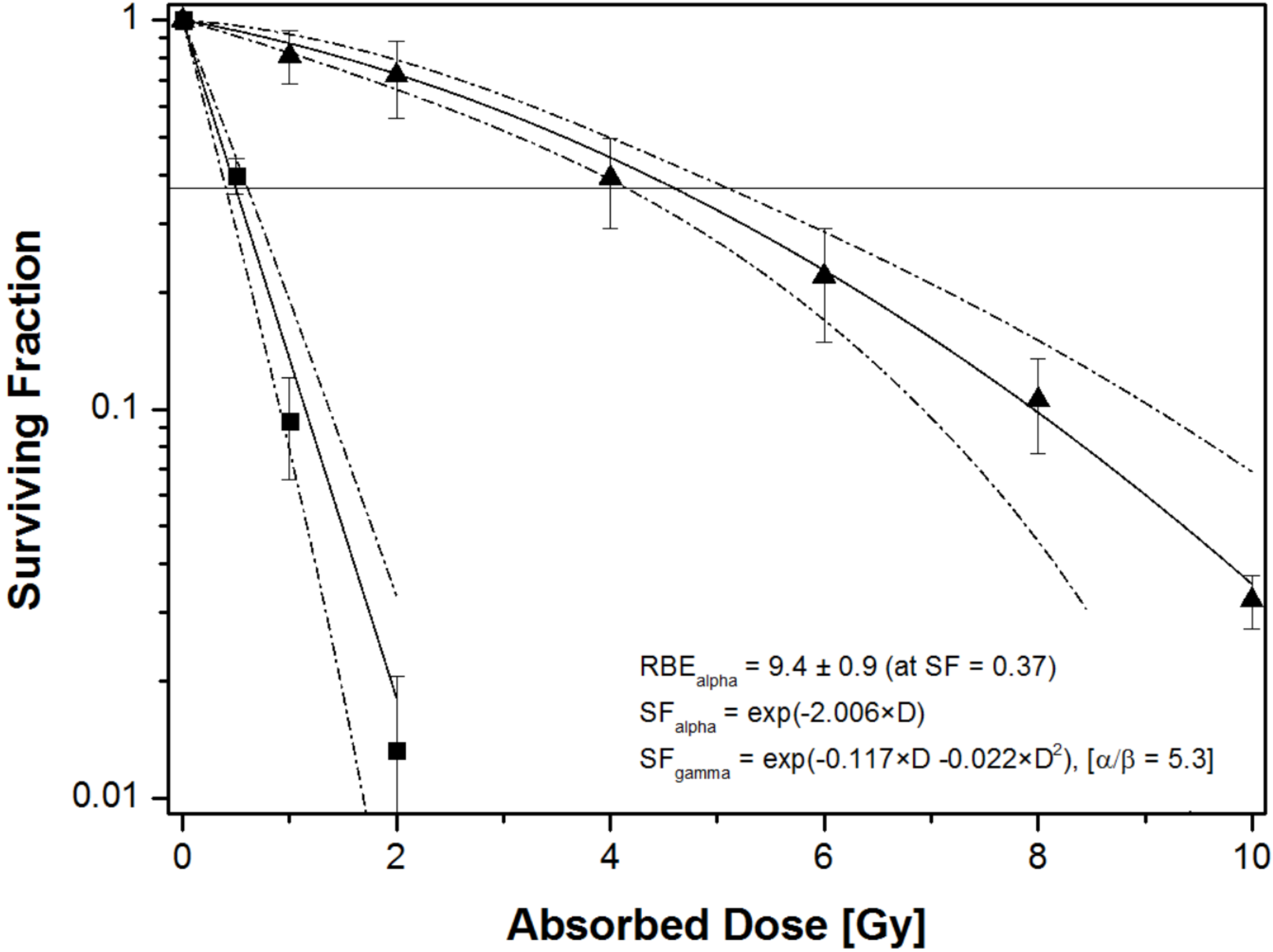
Surviving Fraction
1
0.1
0.01
0
2
4
6
8
10
Absorbed Dose [Gy]
RBE$_{alpha}$ = 9.4 ± 0.9 (at SF = 0.37)
SF$_{alpha}$ = exp(-2.006×D)
SF$_{gamma}$ = exp(-0.117×D -0.022×D^2), [α/β = 5.3]

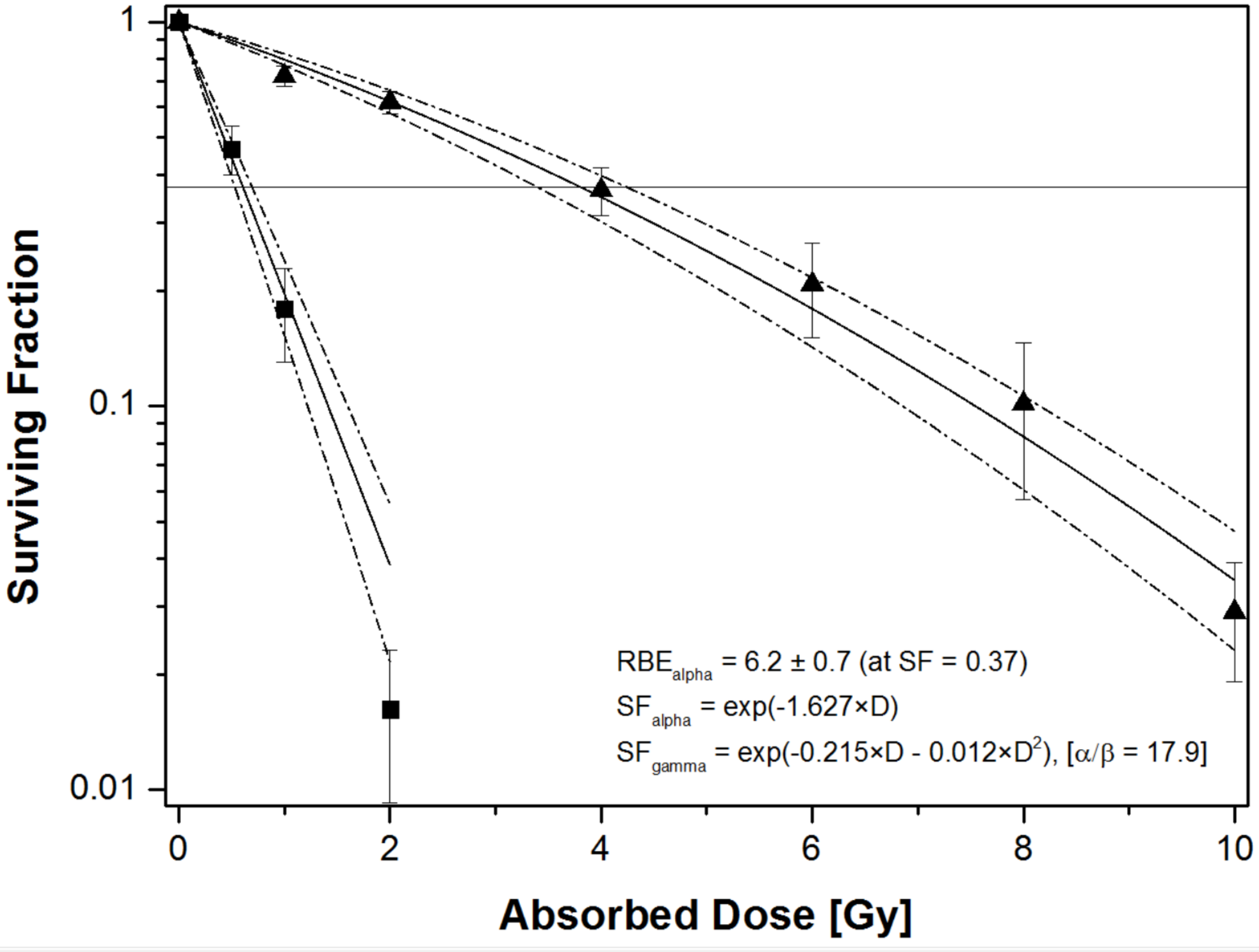
Surviving Fraction
1
0.1
0.01
0
2
4
6
8
10
Absorbed Dose [Gy]
RBE$_{alpha}$ = 6.2 ± 0.7 (at SF = 0.37)
SF$_{alpha}$ = exp(-1.627×D)
SF$_{gamma}$ = exp(-0.215×D - 0.012×D^2), [α/β = 17.9]

TABLE 1. RELATIVE BIOLOGICAL EFFECTIVENESS, SURVIVAL FRACTION AT 2 GRAY FOR BOTH ALPHA PARTICLE AND GAMMA IRRADIATIONS AND THE ALPHA/BETA RATIO FOR THE GAMMA IRRADIATIONS

	RBE	*SF2 (α)*	*SF2 (γ)*	*α/β ratio (γ)*
LNCaP	7.9 ± 1.7	0.03 ± 0.01	0.66 ± 0.12	8.7
DU145	8.0 ± 0.8	0.02 ± 0.01	0.65 ± 0.05	14.2
PC3	7.0 ± 1.1	0.02 ± 0.01	0.62 ± 0.10	17.4
Capan-1	12.5 ± 1.6	< 0.01*	0.61 ± 0.08	15.7
Panc-1	9.4 ± 0.9	0.01 ± 0.01	0.72 ± 0.16	5.3
BxPC-3	6.2 ± 0.7	0.02 ± 0.01	0.62 ± 0.04	17.9

RBE, relative biological effectiveness (mean ± 95% CI) at survival fraction equal to 0.37; SF2 (α), survival fraction at 2 Gy for alpha-particle irradiation (mean ± SD); SF2 (γ), survival fraction at 2 Gy for a gamma irradiation (mean ± SD); α/β ratio (γ), the α/β ratio for the bi-exponential curve fit for the gamma irradiations. *Value not possible to determine since it was lower than the background level.